0026-895X/97/030491-08$3.00/0

MOLECULAR PHARMACOLOGY, **51:**491–498 (1997).

Heteropodatoxins: Peptides Isolated from Spider Venom that Block Kv4.2 Potassium Channels

MICHAEL C. SANGUINETTI,[1] JANICE H. JOHNSON, LANCE G. HAMMERLAND, PAUL R. KELBAUGH, ROBERT A. VOLKMANN, NICHOLAS A. SACCOMANO, and ALAN L. MUELLER

NPS Pharmaceuticals Inc., Salt Lake City, Utah 84108 (M.C.S., J.H.J., L.G.H., A.L.M.), and Pfizer Inc., Groton, Connecticut 06340 (P.R.K., R.A.V., N.A.S.)

Received September 26, 1996; Accepted November 14, 1996

SUMMARY

Toxins isolated from scorpion, snake, and spider venoms are valuable tools to probe the physiologic function and structure of ion channels. In this study, we have isolated three new toxins (heteropodatoxins) from the venom of a spider, *Heteropoda venatoria*. These toxins are structurally similar peptides of 29 to 32 amino acids and share sequence homology with hanatoxins isolated from the venom of a Chilean tarantula. The heteropodatoxins prolonged the action-potential duration of isolated rat ventricular myocytes, suggesting that the peptides block K^+ currents. The effect of toxins on cardiac K^+ currents were studied using voltage clamp techniques. The toxins blocked the transient outward K^+ current but not other K^+ currents in isolated rat cardiac myocytes. The mechanism of block was studied further using Kv4.2, a cloned channel believed to underlie transient outward K^+ current in rat myocytes. The toxins blocked Kv4.2 current expressed in *Xenopus laevis* oocytes in a voltage-dependent manner, with less block at more positive potentials. In addition, the toxins slowed the time course of current activation and inactivation and shifted the voltage dependence of current inactivation to more positive potentials. The heteropodatoxins represent new pharmacologic probes to study the role of Kv4.2 channels in cardiac and neural tissue.

Voltage-sensitive K^+ channels modulate excitability and synaptic transmission of neurons and repolarization of cardiac myocytes. A large number of K^+ channels have been cloned recently, indicating the great diversity of these channels compared with other types of voltage-sensitive channels. The study of their physiologic roles has been aided greatly by the discovery of specific blockers. For example, charybdotoxin isolated from venom of the scorpion, *Leiurus quinquestriatus*, was used to define the function of large conductance Ca^{2+}-activated K^+ channels (1), and the structural determinants of function in *Shaker*-like K^+ channels (2–4). Potassium channel toxins also have been used to distinguish the role of a particular channel type to net current resulting from the overlap of many different types of channels (5, 6) and between different subtypes of a single class of K^+ channels (7).

Transient outward K^+ (I_{to}) channels are characterized by rapid activation and inactivation. These K^+ channels are important in modulation of action-potential configuration and neuronal firing patterns. In the heart, activation of I_{to} channels initiates rapid repolarization of the action potential and is important in regional- and rate-dependent differences in action-potential duration (8). I_{to} channels are blocked by 4-aminopyridine (9), but this compound also blocks other types of K^+ channels (10). Specific blockers of I_{to} channels have not been described.

Two different I_{to} channels have been cloned from cardiac tissue. Kv1.4 (*Shaker* subfamily) and Kv4.2 (*Shal* subfamily) were cloned from heart cDNA libraries, their mRNAs were detected in Northern blots of heart tissue, and have properties similar to voltage-dependent cardiac I_{to} (I_{to1}) when studied in heterologous expression systems (11–13). However, Kv4.2, but not Kv1.4, was detectable in isolated rat myocytes using immunohistochemical techniques (14). These results suggest that Kv4.2 subunits form functional I_{to1} channels in rat heart muscle and that Kv1.4 forms I_{to} channels in other tissues (e.g., neural or smooth muscle) within the heart. Specific blockers of one or both of these channel types would be useful in confirming that Kv4.2 subunits form I_{to1} channels in cardiac myocytes.

In this study, we describe three peptide toxins isolated from the venom of a spider, *Heteropoda venatoria*, that prolong cardiac action potentials and block transient outward K^+ current in rat ventricular myocytes. These peptides (heteropodatoxins) were found to block cloned Kv4.2 (but not Kv1.4) K^+ channels expressed in *X. laevis* oocytes, consistent with the hypothesis that Kv4.2 forms I_{to1} channels in rat heart. The heteropodatoxins will be useful for probing the

[1] Current affiliation: Division of Cardiology, Eccles Program in Human Molecular Biology and Genetics, University of Utah, Salt Lake City, UT 84112.

ABBREVIATIONS: HpTx, heteropodatoxin; I_{to1}, voltage-dependent transient outward potassium current; TFA, trifluoroacetic acid; HPLC, high performance liquid chromatography; PTC, phenylthiocarbamyl.

physiologic role of Kv4.2 K^+ channels and defining the structural basis of Kv4.2 channel function.

Materials and Methods

Isolation/purification of active components from whole venom. *H. venatoria Linneaus* (Araneae, Heteropodidae) were collected from Malaysia and maintained in the vivarium at NPS Pharmaceuticals (Salt Lake City, UT). Whole venom was obtained by electrical stimulation of the cephalothorax of live spiders after anesthetization with CO_2. Whole venom was stored at −80° until used for fractionation. Aliquots of venom (75–120 μl) were diluted to 1 ml with 0.1% aqueous TFA (solution A). The diluted venom was fractionated on a Vydac C-18 reversed-phase HPLC column (10 × 250 mm) equilibrated in 80% A/20% B (0.1% TFA in CH_3CN). After 3 min, the gradient was changed to 24% B over 1 min; at 5 min, a linear gradient from 24 to 35% B over 44 min was begun. The flow rate was 3.5 ml/min and the UV absorbance of the effluent was monitored at 220 nm (Fig. 2A). Fractions were collected and like fractions from the eight chromatographic runs were combined, concentrated by lyophilization, and stored at −80°.

Further purification of fractions 5, 6, and 7 was performed using a HEMA-IEC BIO SB cation-exchange column (10 μm, 4.6 × 150 cm). The lyophilized material was dissolved in 50 mM sodium acetate, pH 4.0, and loaded onto the column. The following gradients were used for elution of the toxins. For reversed-phase fraction 5, which contains $HpTx_1$, the column was developed with a 45-min linear gradient from 0.1 to 1 M NaCl in 50 mM sodium acetate, pH 4.0. $HpTx_1$ eluted between 27 and 34 min. For reversed-phase fraction 6, which contains $HpTx_2$, the column was developed with a 50-min linear gradient from 0 to 0.5 M NaCl in 50 mM sodium acetate. $HpTx_2$ eluted between 27 and 29 min. For reversed-phase fraction 7, which contains $HpTx_3$, the column was developed with a 4-min linear gradient from 0 to 0.3 M NaCl, followed by a 35-min linear gradient from 0.3 to 1.0 M NaCl in 50 mM sodium acetate, pH 4.0. $HpTx_3$ eluted between 30 and 33 min. For each of these chromatographies, the flow rate was 1 ml/min and the effluent was monitored at 280 nm.

The cation-exchange fractions containing $HpTx_1$, $HpTx_2$, and $HpTx_3$ were desalted on a semipreparative Vydac C18 reversed-phase column (10 × 250 mm, 300 Å) equilibrated in 0.1% aqueous TFA (solution A). After loading a cation-exchange fraction onto the column, the column was developed with a 10-min linear gradient from 0 to 25% B (0.1% TFA in acetonitrile), followed by a 20-min linear gradient from 25 to 35% B. The flow rate was 3.5 ml/min and the absorbance of the effluent was monitored at 220 nm. $HpTx_1$ eluted between 24 and 25.5 min, $HpTx_2$ eluted between 26 and 28 min, and $HpTx_3$ eluted between 27 and 29 min. The lyophilized fractions were submitted for amino-terminal sequence and mass spectral analysis.

Mass determination and peptide sequencing. A triple-quadrupole mass spectrometer with an ion-spray interface (SCIEX API III system; Perkin-Elmer, Thornhill, Ontario) was used for mass determination (15). The sample was dissolved in 10% acetic acid and the sample solution (0.2 mg/ml) was delivered at a flow rate of 1.0 μl/min to a sprayer by a syringe infusion pump. The molecular mass of the sample was determined with the first quadrupole, which was calibrated with the ammonium adduct ions of polypropylene glycols.

PTC amino acid analysis was performed on 1–10 nmol of each peptide (in triplicate) with a Waters Pico-Tag system (Waters, Milford, MA). Amino-terminal sequencing was carried out on a pulse-liquid sequenator (Applied Biosystems, Foster City, CA) on both native and *S*-pyridylethylated derivatives. *S*-pyridylethylated peptides were generated *in situ* according to the method of Kruft (16).

Isolation of cardiac myocytes. Adult rats of either sex (200–300 g) were anesthetized with sodium pentobarbital (200 mg/kg, intraperitoneal), then killed by cervical dislocation. The heart was excised rapidly and the aorta was cannulated to an apparatus for retrograde perfusion with oxygenated solutions at 35–36°. The method used to isolate single ventricular myocytes was the same as described previously (17), except that 150 U/ml of collagenase type II (Worthington Biochemicals, Freehold, NJ) and 0.5 units/ml protease type XIV (Sigma Chemical, St. Louis, MO) were used. Myocytes were stored at room temperature in standard extracellular solution before use in voltage clamp experiments.

Whole-cell voltage clamp data acquisition and analysis. The suction microelectrode voltage clamp technique described by Giles and Shibata (18) was used to record currents in single rat ventricular myocytes. Pipettes were fabricated from 1-mm outer-diameter square-bore borosilicate glass (Frederick and Dimmock, Millville, NJ) and had resistances of 3–6 MΩ when filled with an intracellular solution that consisted of 0.5 M potassium gluconate and 25 mM KCl, pH 7.3. Series resistance was compensated by at least 80%. The limitations (high series resistance, loading of cells with K^+ during prolonged recordings) and advantages (no immediate alteration of intracellular contents, ease of seal formation) of using these electrodes and filling solutions has been described previously (19). Command voltage pulses were generated using pClamp software (Axon Instruments, Burlingame, CA), a TL-1 interface (Axon Instruments) connected to a 486DX/50 MHz desktop computer, and an Axoclamp 1D amplifier (Axon Instruments). Currents were low-pass filtered with a cutoff frequency (−3 db) of 1 or 2 kHz.

Rat ventricular myocytes were bathed in a nominally Ca^{2+}-free solution at room temperature. The standard extracellular solution contained 132 mM NaCl, 4 mM KCl, 1 mM $CoCl_2$, 1.2 mM $MgCl_2$, 5 mM HEPES, and 5 mM glucose. The pH was adjusted to 7.2 with NaOH. Currents were elicited with stepped pulses from a holding potential of −60 mV. Each test pulse was preceded by a 20-msec pulse to −30 mV to inactivate I_{Na}. To determine the current-voltage relationship for I_{to1}, pulses were applied every 8 sec in 10-mV increments to test potentials ranging from −40 to +40 mV. This rate of pulsing was sufficiently slow to allow complete recovery of I_{to1} from inactivation at −60 mV between successive test pulses. The magnitude of I_{to1} current was defined as time-dependent current during the 500-msec test pulse. The sustained current (I_{sus}) remaining at the end of the pulse represents a small leak component and a much larger outward K^+ current (20). The voltage dependence of I_{to1} activation was determined from the amplitude of tail currents after 20-msec test pulses. Data was fit with a Boltzmann relation: $I_{to}/I_{to\text{-}max} = 1/(1 + \exp[(V_{1/2} - V_t)/k])$, to estimate the average half-point ($V_{1/2}$) and slope factor (k) for this relationship.

Isolation of oocytes and injection of RNA. *X. laevis* frogs were anesthetized by immersion in 0.2% tricaine for 15–30 min. Ovarian lobes were digested with 2 mg/ml Type 1A collagenase (Sigma Chemical) in Ca^{2+}-free ND96 solution for 1.5 hr to remove follicle cells. Stage IV and V oocytes (21) were injected with Kv4.2 or Kv1.4 cRNA (0.05 mg/ml, 50 nl) and then cultured in Barth's solution supplemented with 50 μg/ml gentamycin and 1 mM pyruvate at 18°. Barth's solution contained 88 mM NaCl, 1 mM KCl, 0.4 mM $CaCl_2$, 0.33 mM $Ca(NO_3)_2$, 1 mM $MgSO_4$, 2.4 mM $NaHCO_3$, 10 mM HEPES, pH 7.4.

Plasmids containing Kv1.4 and Kv4.2 cDNA were kindly provided by Dr. Mike Tamkun (12, 13). Templates for cRNA synthesis from channel DNA were prepared as described by Po *et al.* (13).

Two-microelectrode voltage clamp of oocytes. Oocytes were bathed in ND96 solution. This solution contained 96 mM NaCl, 2 mM KCl, 1 mM $MgCl_2$, 1.8 mM $CaCl_2$, 5 mM HEPES, pH 7.6. Currents were recorded at room temperature (21–23°) using standard two-microelectrode voltage clamp techniques. Glass microelectrodes were filled with 3 M KCl and their tips were broken to obtain tip resistances of 1–3 MΩ for the voltage-recording electrode and 0.6–1 MΩ for the current-passing electrode. Oocytes were voltage clamped with an Axoclamp 2A amplifier (Axon Instruments). Voltage commands were generated using pCLAMP software (version 5.5; Axon Instruments), a 486DX2 personal computer, and a Digidata 1200 D/A interface (Axon Instruments). Current signals were sampled digitally at a rate equal to 2–4 times the low-pass cutoff frequency (−3 db) of an 8-pole

Bessel filter. The oocyte membrane potential was maintained at −70 mV between test pulses, applied at a rate of 1–3 pulses/min.

The time course of Kv4.2 inactivation was fit with a single exponential relationship: $I(t) = A_0 + A_{1e}^{(-t/\tau)}$, using a Chebyshev noniterative fitting technique (pCLAMP). The voltage dependence of Kv4.2 inactivation was determined using 8-sec conditioning test pulses applied once every 30 sec. Each conditioning pulse was applied to a potential ranging from −120 to 0 mV and was followed by a pulse to +40 or +75 mV to monitor the extent of channel inactivation.

Data analyses, including exponential fitting of current traces, were performed using pCLAMP. Fits of appropriate data to a Boltzmann function or Hill equation were performed using Kaleidagraph (Synergy Software, Reading, PA). Data are expressed as the mean ± standard error.

Results

Effects of whole venom on cardiac myocytes. We determined the effects of whole venom (1:2000 dilution) on K^+ current in isolated rat ventricular myocytes. As shown in Fig. 1, the venom decreased the amplitude of I_{to1} in a voltage-dependent manner, with relief of block at the most positive test potentials. I_{to1} was completely blocked at test potentials between −30 and +10 mV, 53% decreased at +30 mV, and only 2% decreased at +60 mV.

Isolation, purification, and amino acid sequence of active components from whole venom. Fractionation of *H. venatoria* whole venom on a Vydac C-18 reversed-phase HPLC column revealed several prominent peaks as detected by UV absorbance at 220 nm (Fig. 2). Eight fractions, as indicated in Fig. 2A, were collected, lyophilized, and stored at −80°. Each fraction was diluted with 1 ml of H_2O and tested at a 1:100 dilution of this stock solution for effects on I_{to1} in isolated myocytes. Peaks 2 and 5–8 completely blocked I_{to1} measured at −10 mV. Three of these fractions (5–7) were chosen for further characterization. Peak 5 eluted from the reversed-phase column between 27 and 30 min, peak 6 eluted between 30 and 33.5 min, and peak 7 eluted between 33.5 and 37 min. These fractions were further purified by cation-exchange and reversed-phase chromatography as described in Materials and Methods.

Mass spectral analysis of the HpTx was obtained using a SCIEX API III ion-spray mass spectrometer. The observed mass of $HpTx_1$, $HpTx_2$, and $HpTx_3$ were 3910.57, 3412.72, and 3599.38, respectively. The peptides all had amides on their carboxyl termini. The amino acid sequences of the purified toxins, $HpTx_1$, $HpTx_2$, and $HpTx_3$, were determined by amino-terminal sequencing and are shown in Fig. 2B. Amino acid identity was 39–41% among the HpTxs. $HpTx_3$ is also 39% identical to $hanatoxin_2$, a peptide toxin isolated from a Chilean tarantula, *Grammostola spatulata* (22).

$HpTx_2$ prolongs action potential duration and blocks transient outward current in rat cardiac myo-

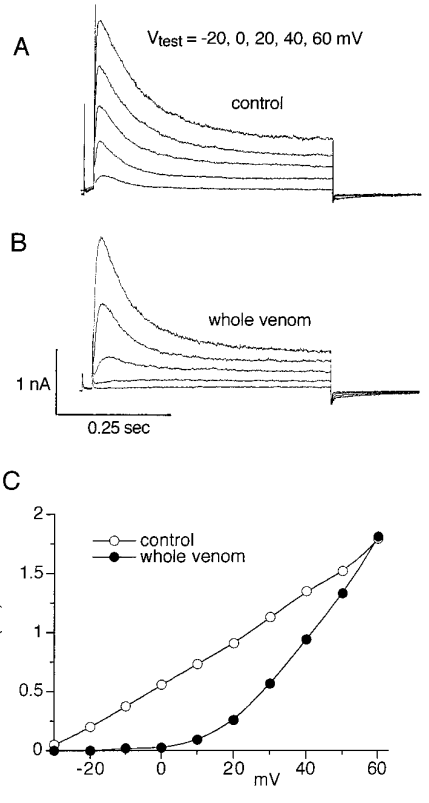

Fig. 1. *H. venatoria* venom causes voltage-dependent block of I_{to1} in isolated rat ventricular myocyte. Cell was exposed to 1:2000 dilution of whole venom. A and B, Currents were elicited from a holding potential of −50 mV. A brief prepulse to −30 mV was followed by 0.5-sec pulses to the indicated test potentials. C, Block of I_{to1} by venom was decreased as the test potential was increased.

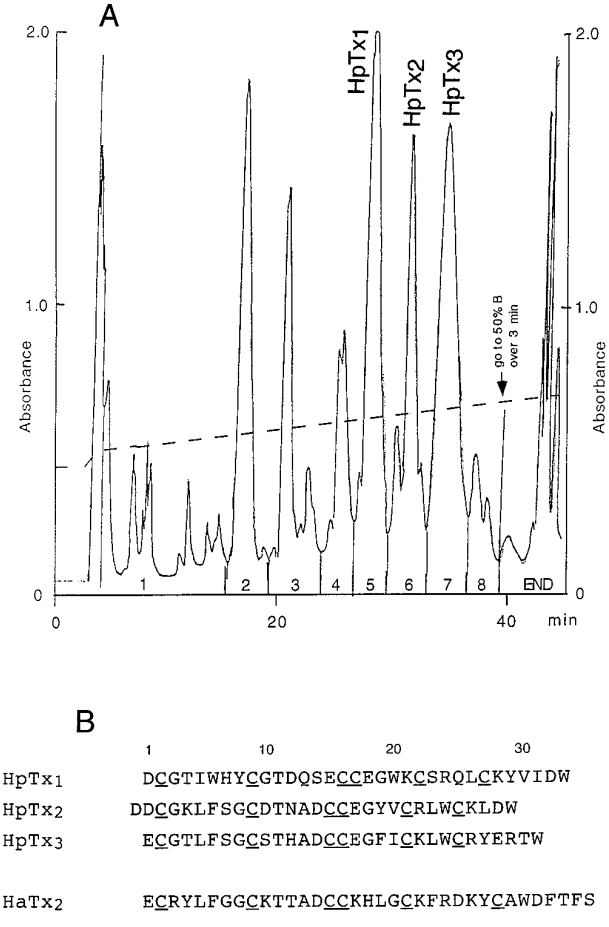

Fig. 2. Reversed-phase HPLC chromatogram of *H. venatoria* venom and sequence of HpTxs. A, Venom (120 μl) was dissolved in 0.1% TFA (aq) and applied to a Vydac C-18 column as described in Materials and Methods. UV absorbance of the effluent was monitored at 220 nm. Fractions were collected as noted on the chromatogram. B, Sequences of HpTxs and comparison to $hanatoxin_2$ (22).

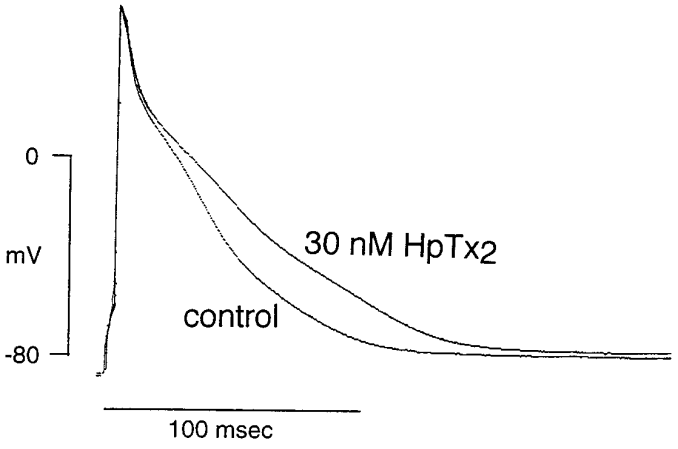

Fig. 3. Prolongation of action potential in an isolated rat ventricular myocyte by 30 nM $HpTx_2$.

cytes. Isolated rat ventricular myocytes were current clamped and stimulated with suprathreshold current pulses (2-msec duration) at a frequency of 0.2 Hz to elicit action potentials. Action potential duration was measured at 90% repolarization, which was prolonged immediately after addition of $HpTx_2$ to the cell chamber, and reached a steady state within 1 min thereafter. $HpTx_2$ (30 nM) lengthened 90% repolarization by 34 ± 5% (n = 5; Fig. 3).

$HpTx_2$ blocked I_{to1} but had no effect on the inward rectifier K^+ current (I_{K1}), L-type Ca^{2+} current, or the maintained outward current (I_{sus}). The block of I_{to} was voltage-dependent; less block was apparent at more positive membrane potentials. For example, 1 μM $HpTx_2$ completely blocked I_{to1} at a test potential of −10 mV (Fig. 4A) but decreased peak I_{to1} by less than 50% at a test potential of +30 mV (Fig. 4, B and C). $HpTx_2$ had no effect on I_{sus}, a very rapidly activating delayed rectifier K^+ current (20) (Fig. 4D). The voltage-dependent block of I_{to} by $HpTx_2$ results in a shift in the voltage dependence of current activation. In the example shown in Fig. 5A, the half-point for I_{to} activation was −13 mV in control and 6 mV after treatment of the cell with 30 nM $HpTx_2$. The slope factor for the activation curve was increased from 5 mV in control to 12 mV after toxin.

The concentration-dependent block of I_{to1} by $HpTx_2$ was determined at three different test potentials (Fig. 5B). The concentration required for 50% block (IC_{50}) at a test potential of −10 mV was 15.8 ± 0.6 nM, with complete block at about 100 nM. The Hill coefficient for the concentration-effect curve was 2.1. At +20 and +50 mV, block was incomplete. Therefore, the IC_{50} value and the concentration required for half-maximal block ($IC_{50\text{-max}}$) were determined. The IC_{50} values were 35 and 138 nM at +20 and +50 mV, respectively. The $IC_{50\text{-max}}$ value was 24 ± 1.5 nM (Hill coefficient = 1.5) at +20 mV and 34 ± 11.5 nM (Hill coefficient = 1.0) at +50 mV. The decrease of I_{to} block at more positive test potentials suggests that depolarization causes dissociation of the toxin from its receptor.

Preliminary experiments have shown that $HpTx_2$ (0.2–1 μM) did not have any effect on delayed rectifier K^+ currents recorded from rat neurons (cerebellar granule, Purkinje, sympathetic ganglion cells), GH_3 pituitary cells, or rabbit osteoclasts (data not shown).

HpTxs block Kv4.2 channels. Two types of transient outward K^+ channels have been cloned from rat heart cDNA libraries, Kv1.4 and Kv4.2 (11, 12). We tested the effects of the toxins on these two cloned K^+ channels expressed in *X.*

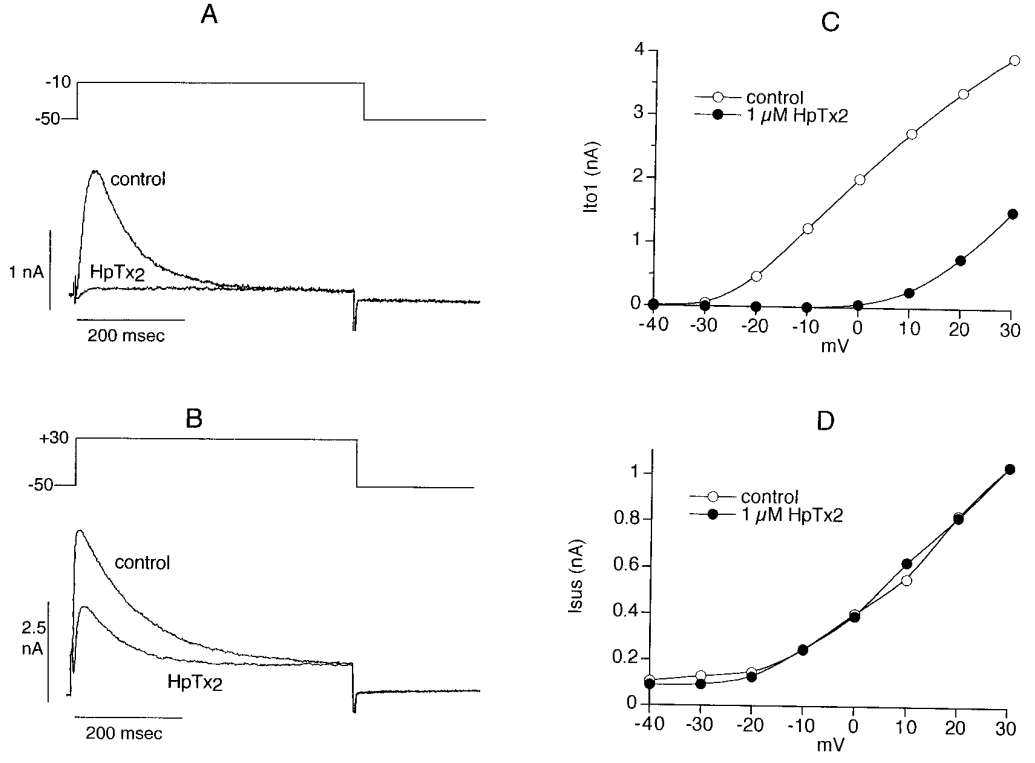

Fig. 4. Voltage-dependent block of I_{to1} in isolated rat ventricular myocyte by $HpTx_2$. A and B, Current recorded at a test potential of −10 mV was completely blocked by 1 μM $HpTx_2$, but current recorded at +30 mV was only blocked by ~50%. C, Voltage-dependent block of I_{to1} by 1.0 μM $HpTx_2$. D, $HpTx_2$ had no effect on I_{sus}.

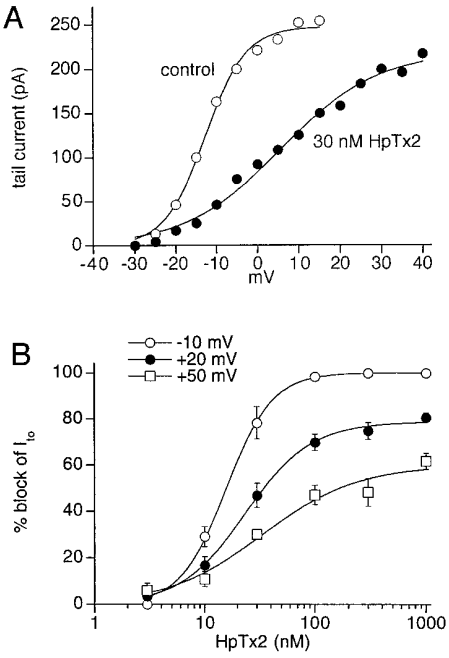

Fig. 5. Voltage-dependent effects of HpTx2 on I_{to} in isolated rat ventricular myocyte. A, $HpTx_2$ shifts the voltage dependence of I_{to1} activation. Curves represent best fits of the data to a Boltzmann function; control: $V_{1/2}$ = −13 mV, slope = 5 mV; 30 nM $HpTx_2$: $V_{1/2}$ = 6 mV, slope = 12 mV. B, Voltage- and concentration-dependent block of I_{to1} by $HpTx_2$ in isolated rat ventricular myocytes. Block was determined at test potentials of −10, +20, and +50 mV (n = 5). Each curve represents a fit of the data to a Hill equation.

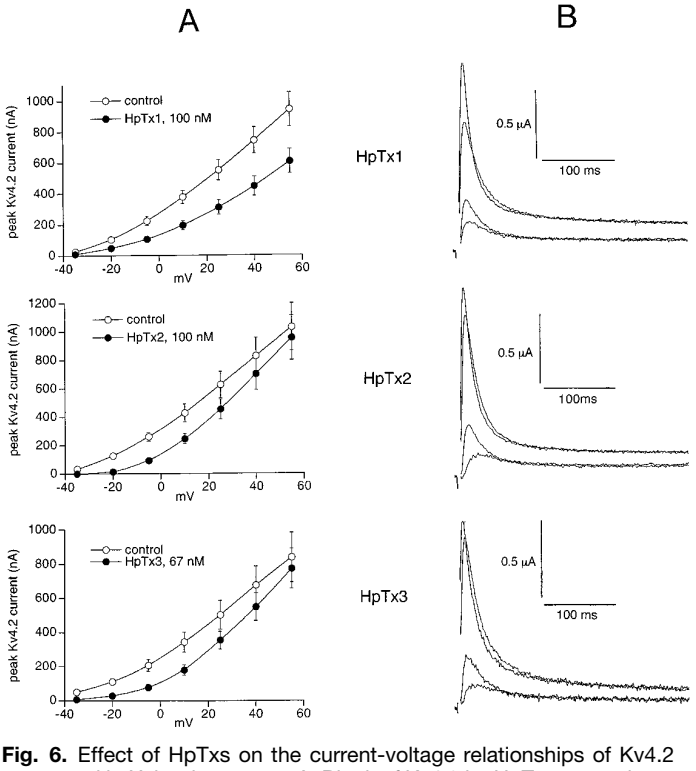

Fig. 6. Effect of HpTxs on the current-voltage relationships of Kv4.2 expressed in *X. laevis* oocytes. A, Block of Kv4.2 by HpTxs was voltage dependent (n = 4 for each toxin). B, Examples of Kv4.2 currents recorded at test potentials of −5 and +55 mV, before and after exposure of different oocytes to each HpTx at the concentration indicated in A.

laevis oocytes. $HpTx_2$ and $HpTx_3$, at a concentration of 2 µM, had no effect on Kv1.4 (not shown). All three HpTxs blocked Kv4.2 in a concentration-dependent manner. For example, at a test potential of −5 mV, $HpTx_3$ decreased Kv4.2 84% at 400 nM, 72% at 200 nM, and 58% at 67 nM (n = 4). The voltage dependence of block of Kv4.2 was determined using a concentration of toxin that decreased current by 50% at a test potential near 0 mV (100 nM for $HpTx_1$ and $HpTx_2$, and 67 nM for $HpTx_3$). The current-voltage relationships for Kv4.2 determined before and after exposure to each HpTx are shown in Fig. 6. The voltage dependence of block was linear for 100 nM $HpTx_1$ and 67 nM $HpTx_3$ (Fig. 7A) but was curvilinear for 100 nM $HpTx_2$ (Fig. 7B). The data for $HpTx_2$ was well described with the sum of a linear component and a sigmoidal component fit with a Boltzmann function. From these data, the voltage at which Kv4.2 was blocked by 50% was determined to be +4 mV for all three toxins.

The toxins increased the time required for currents to reach peak amplitude (Fig. 8A) and decreased the rate of current inactivation (Fig. 8B). The effect of $HpTx_3$ on the voltage-dependence of current inactivation was determined. For these experiments, the holding potential was −90 or −100 mV. An 8-sec conditioning prepulse was applied to potentials ranging from −120 to 0 mV. After each conditioning prepulse, a test pulse was applied to +40 mV in one group

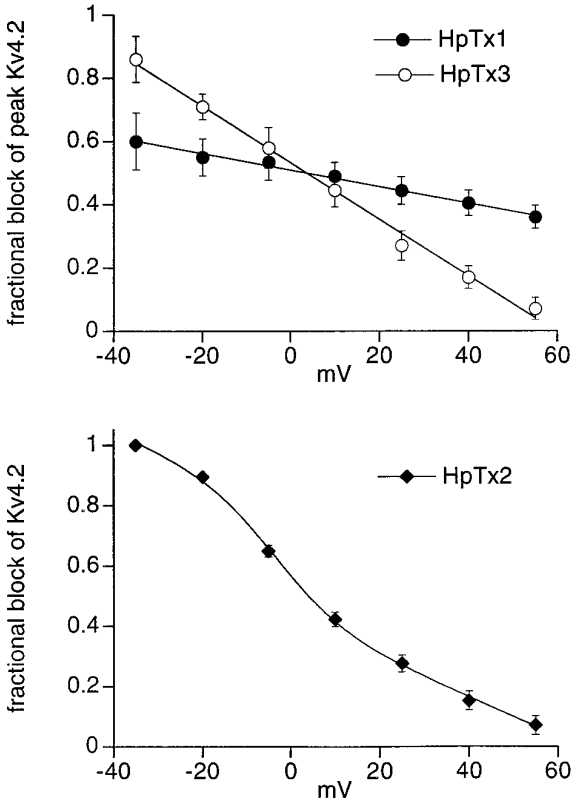

Fig. 7. Voltage-dependent block of Kv4.2 expressed in *X. laevis* oocytes by HpTxs. The relationship between fractional block of current and test potential was determined with 100 nM $HpTx_1$ and $HpTx_2$ and with 67 nM $HpTx_3$ (n = 4 for each toxin). The data for $HpTx_1$ were best fit with the linear function: fractional block (B_f) = −0.00262 mV + 0.510. The data for $HpTx_3$ were also best fit with a linear function: B_f = −0.00895 mV + 0.533. The data for $HpTx_2$ were best fit with the sum of a Boltzmann and a linear function: B_f = 0.367/[1 + exp((V_t + 3.29)/7.85)] − 0.0065 mV + 0.422.

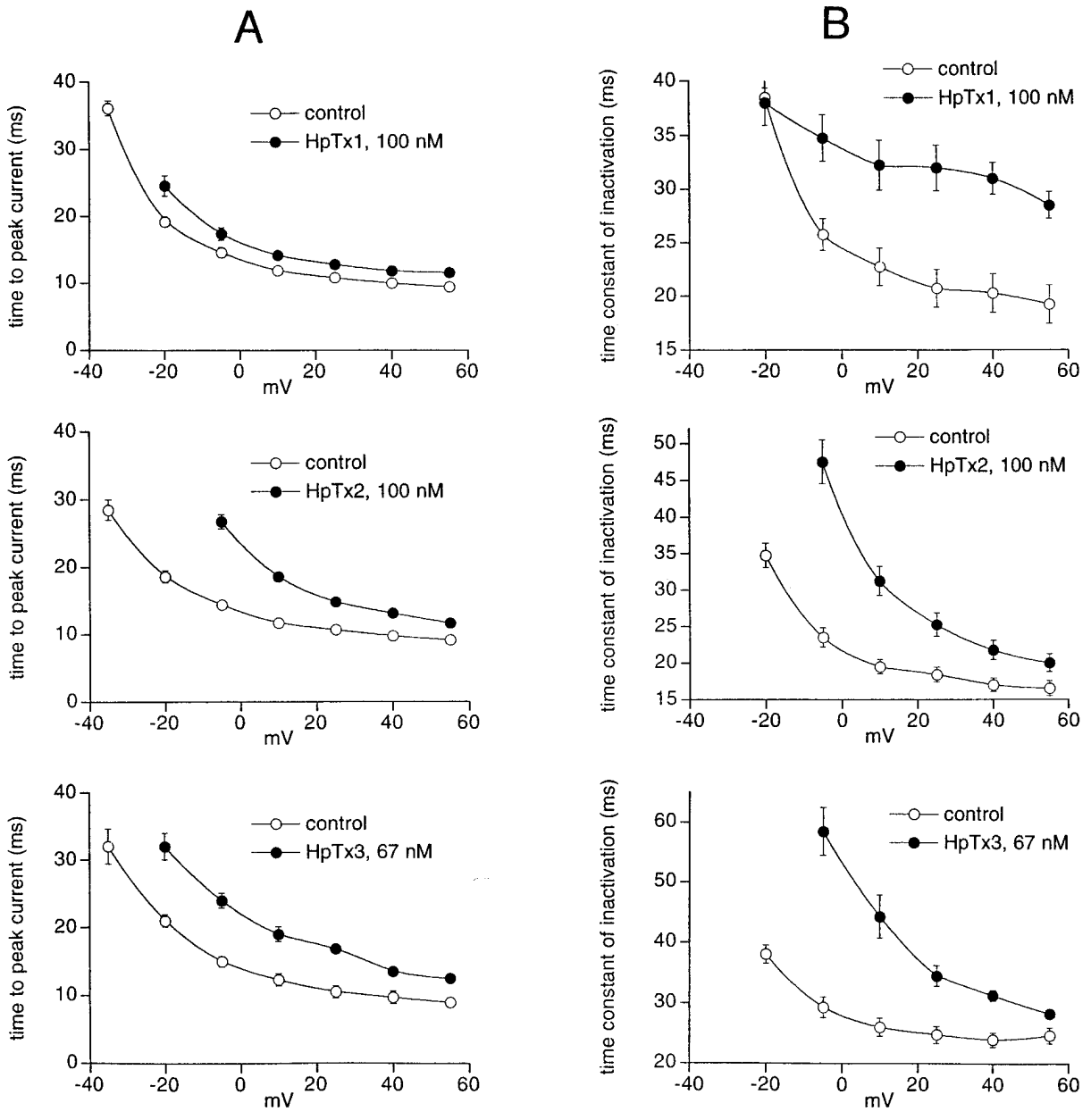

Fig. 8. Effect of HpTxs on the rate of activation and inactivation of Kv4.2 expressed in *X. laevis* oocytes. A, Time to peak outward current is slowed by HpTxs (n = 4). B, The time constant of current inactivation is slowed by HpTxs (n = 4).

of oocytes. In another set of oocytes, a test potential to +75 mV was used to assess current inactivation. When the test pulse was applied to +40 mV, the steady-state inactivation curves were fit with a Boltzmann function and had an average half-point ($V_{1/2}$) of −67.6 ± 0.9 mV and a slope factor of 6.4 ± 0.2 mV (n = 4) under control conditions. In the presence of 100 nM $HpTx_3$, the $V_{1/2}$ was −59.5 ± 2.6 mV and the slope factor was 9.6 ± 0.8 mV. Using this pulse protocol, the inactivation curves overlapped; the test current in the presence of toxin was smaller when the conditioning pulse was applied to a voltage lower than −55 mV. However, when the conditioning pulse was applied to voltages higher than −55 mV, the test current was larger in the presence of $HpTx_3$ than in control (Fig. 9A). When a test pulse to +75 mV was used to assess the extent of channel inactivation, control data was still best fit with a Boltzmann function. The average $V_{1/2}$ was −68.3 ± 0.8 mV, and the slope factor was 8.4 ± 1.4 mV (n = 4). After exposure to 100 nM $HpTx_3$, the inactivation curve had a similar maximum value (due to relief of block) but was shifted to a more positive potential (Fig. 9B). The voltage dependence of inactivation in the presence of toxin did not have a simple sigmoidal shape and was not well described with a single Boltzmann function. However, the data were best fit with a sum of two Boltzmann functions. For these fits, the values for $V_{1/2}$ and the slope for one of the Boltzmann functions was fixed at the values measured from the matching control experiment. The second Boltzmann component had an average $V_{1/2}$ of −39.8 ± 2.7 mV and a slope factor of 7.3 ± 0.3 mV (n = 4). The relative amplitude of the second component was 0.69 ± 0.03. These results suggest that approximately 70% of the channels were bound by $HpTx_3$ and inactivated with an altered voltage dependence.

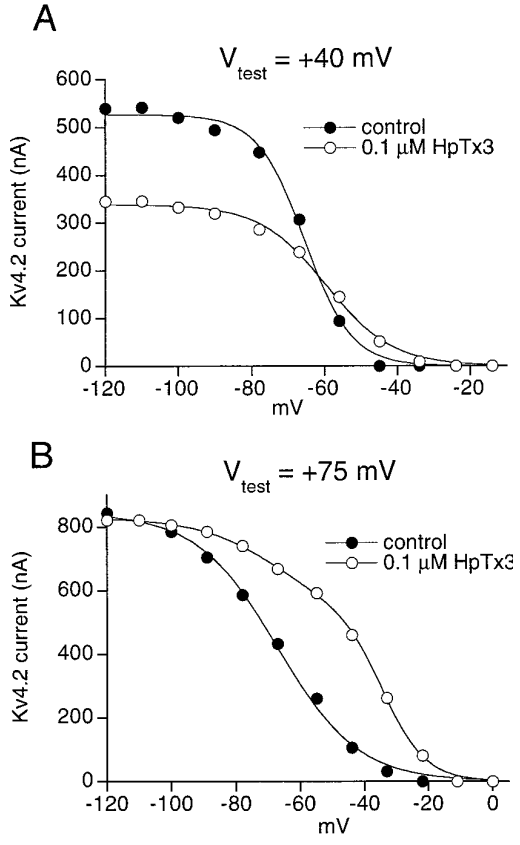

Fig. 9. $HpTx_3$ shifts the voltage dependence of Kv4.2 inactivation. A, Inactivation assessed with a test pulse to +40 mV. Smooth curves are best fits of the data to a Boltzmann function. In control, $V_{1/2}$ was −65.5 mV and the slope factor was 6.4 mV. In the presence of $HpTx_3$, $V_{1/2}$ was −59.6 mV and the slope factor was 9.1 mV. B, Inactivation assessed with a test pulse to +75 mV in another oocyte. In control, $V_{1/2}$ was −67.0 mV and the slope factor was 12.5 mV. In the presence of $HpTx_3$, the data were fit with the sum of two Boltzmann functions. The $V_{1/2}$ and slope factor for one component were fixed at the values determined in control; the other component had a $V_{1/2}$ of −34.2 mV and a slope factor of 6.5 mV.

Discussion

Our discovery of K^+ channel blockers from the venom of *H. venatoria* is the latest of several recent reports demonstrating that spider venom is a rich source of ion channel modulators. Toxins have been isolated that block voltage-dependent Ca^{2+} and K^+ channels and glutamate receptor-operated channels. The ω-agatoxins (ω-Aga-1A–IVA) are peptide toxins isolated from the funnel web spider, *Agelenopsis aperta,* that block N-, P-, and L-type Ca^{2+} channels (23, 24). Related toxins isolated from the Chilean tarantula, *G. spatulata* (ω-grammotoxin) and *Hololena curta* (Hololena toxin), also block Ca^{2+} channels (25, 26). Acylpolyamine toxins isolated from the venom of orb weaver spiders (*Argiope* sp.) and *A. aperta* block glutamate receptor-operated channels (27). Most recently, peptides (hanatoxins) were isolated from the venom of *G. spatulata* that block the Kv2.1 K^+ channel expressed in *X. laevis* oocytes (22). It is likely that spider venoms will yield many more interesting and useful ion channel modulators.

We found that the voltage dependence of Kv4.2 block varied among the three different HpTxs. Block was less voltage dependent for $HpTx_1$ than for $HpTx_2$ and $HpTx_3$. The block of Kv4.2 by $HpTx_1$ and $HpTx_3$ was a linear function of voltage, whereas block by $HpTx_2$ was a curvilinear function of voltage. The mechanisms of channel block by these toxins is not known. The strong voltage dependence of block is consistent with relief of block upon depolarization. This could result either from dissociation of the toxin from a binding site in or near the pore caused by outward flow of K^+ and/or from a modulation of intrinsic channel-gating behavior.

It is often difficult to correlate channel activity recorded from isolated cells with specific channel types cloned from the the same tissue. Relatively specific pharmacologic probes can help resolve this difficulty. For example, it was suggested that Kv1.4 K^+ channels may contribute to I_{to1} in cardiac ventricular myocytes (13). However, despite some similarities, some biophysical properties of these channels are significantly different. The rate of activation and inactivation and the sensitivity to block by 4-aminopyridine were similar for human Kv1.4 and human I_{to1}, but the recovery from inactivation was slower, and the half-point of activation and inactivation were more negative for Kv1.4 than for I_{to1} in isolated myocytes (13). Our finding that HpTxs block Kv4.2, but not Kv1.4, suggests that I_{to1} in rat myocytes is formed from Kv4.2 and not from Kv1.4 channel subunits.

$Hanatoxin_1$ and $hanatoxin_2$ share significant sequence homology with the HpTxs (Fig. 2B). The hanatoxins were reported to block Kv2.1 with an IC_{50} value of 42 nM. $Hanatoxin_1$ (500 nM) also blocked Kv4.2 by 73% at a test potential of 0 mV. Block of Kv4.2 by hanatoxin was characterized by a slowed time to peak and a slowed rate of inactivation, similar to the pattern of block of Kv4.2 by the HpTxs. Although the voltage dependence of Kv4.2 block was not investigated, considering these characteristics of block and similarity in sequence to the HpTxs, it is likely that the hanatoxins will also block Kv4.2 in a voltage-dependent manner. Future experiments are needed to determine whether HpTxs also block Kv2.1.

In situ hybridization of rat brain has shown that Kv4.2 channels are strongly expressed in the cerebellum and hippocampus, especially in the dentate gyrus and the pyramidal cells of the CA3 and CA1 region (28). The level of Kv4.2 mRNA in the excitatory dentate granule cell layer was downregulated after seizure activity induced with a single dose of pentylenetetrazol in rats. Repression of Kv4.2 channel gene expression may enhance synaptic activity and may be involved in phenomenon such as kindling, a long-lasting epileptic state centered in the hippocampus (28). The HpTxs probably will be useful pharmacologic tools to determine the role of Kv4.2 channel activity in normal and pathological neural activities.

In summary, we have isolated several related peptide toxins from venom of *H. venatoria* that block I_{to1} in isolated cardiac myocytes and Kv4.2 channels expressed in *X. laevis* oocytes. The heteropodatoxins represent a new class of modulators that will be useful in defining the physiologic role of Kv4.2 channels in a variety of cell types and will aid in structure function studies of these channels.

Acknowledgments

We thank C. Levinthal for collection of spiders, R. Roeloffs for collection of venom, and J. Busby and J. Garrett for synthesis of cRNA. Mass spectral analysis was performed by Y. Konishi at the Biotechnology Research Institute (Montreal, Quebec, Canada).

References

1. Robitaille, R., M. Garcia, G. J. Kaczorowski, and M. P. Charlton. Functional colocalization of calcium and calcium-gated potassium channels in control of transmitter release. *Neuron* **11:**645–655 (1993).
2. MacKinnon, R., and C. Miller. Mutant potassium channels with altered binding of charybdotoxin, a pore-blocking peptide inhibitor. *Science (Washington D. C.)* **245:**1382–1385 (1989).
3. MacKinnon, R. Determination of the subunit stoichiometry of a voltage-activated potassium channel. *Nature (Lond.)* **350:**232–235 (1991).
4. Goldstein, S. A. N., D. J. Pheasant, and C. Miller. The charybdotoxin receptor of a *Shaker* K^+ channel: peptide and channel residues mediating molecular recognition. *Neuron* **12:**1377–1388 (1994).
5. Moczydlowski, E., K. Lucchesi, and A. Ravindran. An emerging pharmacology of peptide toxins targeted against potassium channels. *J. Membr. Biol.* **105:**95–111 (1988).
6. Strong, P. N. Potassium channel toxins. *Pharmacol. Ther.* **46:**137–162 (1990).
7. Benoit, E., and J. M. Dubois. Toxin 1 from the snake Dendroaspis polyepsis: a highly specific blocker of one type of potassium channel in myelinated nerve fibre. *Brain Res.* **377:**374–377 (1986).
8. Fedida, D., and W. R. Giles. Regional variations in action potentials and transient outward current in myocytes isolated from rabbit left ventricle. *J. Physiol. (Lond.).* **442:**191–209 (1991).
9. Kenyon, J. L., and W. R. Gibbons. 4-aminopyridine and the early outward current of sheep cardiac Purkinje fibers. *J. Gen. Physiol.* **73:**139–157 (1979).
10. Van Bogaert, P. P., and D. J. Snyders. Effects of 4-aminopyridine on inward rectifying and pacemaker currents of cardiac Purkinje fibres. *Pfluegers Arch. Eur. J. Physiol.* **394:**230–238 (1982).
11. Roberds, S. L., and M. M. Tankun. Cloning and tissue-specific expression of five voltage-gated potassium channel cDNAs expressed in rat heart. *Proc. Natl. Acad. Sci. USA* **88:**1798–1802 (1991).
12. Blair, T. A., S. L. Roberds, M. M. Tamkun, and R. P. Hartshorne. Functional characterization of RK5, a voltage-gated K^+ channel cloned from the rat cardiovascular system. *FEBS Lett.* **295:**211–213 (1991).
13. Po, S., D. J. Snyders, R. Baker, M. M. Tamkun, and P. B. Bennett. Functional expression of an inactivating potassium channel cloned from human heart. *Circ. Res.* **71:**732–736 (1992).
14. Barry, D. M., J. S. Trimmer, J. P. Merlie, and J. M. Nerbonne. Differential expression of voltage-gated K^+ channel subunits in adult rat heart. Relation to functional channels? *Circ. Res.* **77:**361–369 (1995).
15. Feng, R., Y. Konishi, and A. W. Bell. High accuracy molecular weight determination and variation characterization of proteins up to 80 KU by ionspray mass spectrometry. *J. Am. Soc. Mass Spectrom.* **2:**387–401 (1991).
16. Kruft, V. On-sequencer pyridylethylation of cysteine residues after protection of amino groups by reaction with phenyl isothiocyanate. *Anal. Biochem.* **193:**306 (1991).
17. Kamp, T. J., M. C. Sanguinetti, and R. J. Miller. Voltage- and use-dependent modulation of cardiac calcium channels by the dihydropyridine (+)-202–791. *Circ. Res.* **64:**338–351 (1989).
18. Giles, W. R., and E. F. Shibata. Voltage clamp of bull-frog cardiac pacemaker cells: a quantitative analysis of potassium currents. *J. Physiol. (Lond).* **368:**265–292 (1985).
19. Jurkiewicz, N. K., and M. C. Sanguinetti. Rate-dependent prolongation of cardiac action potentials by a methanesulfonanilide class III antiarrhythmic agent: specific block of rapidly activating delayed rectifier K^+ current by dofetilide. *Circ. Res.* **72:**75–83 (1993).
20. Apkon, M., and J. M. Nerbonne. Characterization of two distinct depolarization-activated K^+ currents in isolated adult rat ventricular myocytes. *J. Gen. Physiol.* **97:**973–1011 (1991).
21. Dumont, J. N. Oogenesis in *Xenopus laevis* (Daudin). *J. Morphol.* **136:**153–180 (1972).
22. Swartz, K. J., and R. MacKinnon. An inhibitor of the Kv2.1 potassium channel isolated from the venom of a chilean tarantula. *Neuron* **15:**941–949 (1995).
23. Olivera, B. M., G. P. Miljanich, J. Ramachandran, and M. E. Adams. Calcium channel diversity and neurotransmitter release: the w-conotoxins and w-agatoxins. *Annu. Rev. Biochem.* **63:**823–867 (1994).
24. Bindokas, V. P., and M. E. Adams. ω-Aga-1: a presynaptic calcium channel antagonist from venom of the funnel web spider, Agelenopsis aperta. *J. Neurobiol.* **20:**171–188 (1989).
25. Lampe, R. A., P. A. Defeo, M. D. Davison, J. Young, J. L. Herman, R. C. Spreen, M. B. Horn, T. J. Mangano, and R. A. Keith. Isolation and characterization of ω-grammotoxin SIA, a novel peptide inhibitor of neuronal voltage-sensitive calcium channel responses. *Mol. Pharmacol.* **44:**451–460 (1993).
26. Leung, H. -T., and L. Byerly. Characterization of single calcium channels in Drosophila embryonic nerve and muscle cells. *J. Neurosci.* **11:**3047–3059 (1991).
27. Parks, T. N., A. L. Mueller, L. D. Artman, B. C. Albensi, E. F. Nemeth, H. Jackson, V. J. Jasys, N. A. Saccomano, and R. A. Volkmann. Arylamine toxins from funnel-web spider (Agelenopsis aperta) venom antagonize *N*-methyl-D-aspartate receptor function in mammalian brain. *J. Biol. Chem.* **266:**21523–21529 (1991).
28. Tsaur, M. -L., M. Sheng, D. H. Lowenstein, Y. N. Jan, and L. Y. Jan. Differential expression of K^+ channel mRNAs in the rat brain and down-regulation in the hippocampus following seizures. *Neuron* **8:**1055–1067 (1992).

Send reprint requests to: Michael Sanguinetti, Ph.D., Division of Cardiology, University of Utah, Bldg. 533, Room 4220, Salt Lake City, UT 84112.